Available online at www.sciencedirect.com
ScienceDirect
Chemical Engineering and Processing 46 (2007) 1067–1084
Chemical Engineering and Processing Process Intensification
www.elsevier.com/locate/cep

Efficient optimization of simulated moving bed processes

A. Toumi [a], S. Engell [a], M. Diehl [b,*], H.G. Bock [b], J. Schlöder [b]

[a] *Department of Chemical and Biochemical Engineering, Universität Dortmund, Germany*
[b] *Interdisciplinary Center for Scientific Computing, Universität Heidelberg, Germany*

Accepted 21 June 2006
Available online 16 March 2007

Abstract

Simulated moving bed (SMB) chromatography is attracting more and more attention since it is a powerful technique for complex separation tasks. Nowadays, more than 60% of preparative SMB units are installed in the pharmaceutical and in the food industry [SDI, Preparative and Process Liquid Chromatography: The Future of Process Separations, International Strategic Directions, Los Angeles, USA, 2002. http://www.strategic-directions.com]. Chromatography is the method of choice in these fields, because often pharmaceuticals and fine-chemicals have physico-chemical properties which differ little from those of the by-products, and they may be thermally instable [J. Kinkel, M. Schulte, R. Nicoud, F. Charton, Simulated moving bed (SMB) chromatography: an efficient method for performing large-scale separation of optical isomers, Chiral Eur. 95 (1995) 121–132; J. Strube, A. Jupke, A. Epping, H. Schmidt-Traub, M. Schulte, R. Devant, Design, optimization and operation of chromatographic processes in the production of enantiomerically pure pharmaceuticals, Chirality 11 (1999) 440–450]. In these cases, standard separation techniques as distillation and extraction are not applicable [S. Imamoglu, Simulated moving bed chromatography (SMB) for applications in bioseparation, Adv. Biochem. Eng. Biotechnol. 76 (2002) 211–231]. The use of the SMB technology leads to more efficient operations in terms of dilution and adsorbent utilization than the classical batch separation.

Optimization of SMB processes is still a challenging task, particularly when a rigorous first-principles process model is used. SMB processes exhibit strong non-linear behavior and they are of periodic nature. Additionally, their hybrid, non-steady and non-ideal characteristics have to be taken into account. Model-based optimization strategies are therefore of great importance for research and practice. In this article, we report new efficient numerical approaches for the solution of the dynamic optimization problem arising from SMB processes [A. Toumi, Optimaler Betrieb und Regelung von Simulated Moving Bed Prozessen, Dissertation, Fachbereich Bio und Chemieingenieurwesen, University of Dortmund, 2004]. They have been developed in the software package MUSCOD-II [D. Leineweber, Efficient reduced SQP methods for the optimization of chemical processes described by large sparse DAE models, Dissertation, vol. 613, VDI Reihe 3, Verfahrenstechnik, VDI Verlag, 1999], a recent implementation of the direct multiple shooting method where the optimal state trajectory and the corresponding operating parameters are determined simultaneously [H. Bock, K. Plitt, A multiple shooting algorithm for direct solution of optimal control problems, in: Proceedings of the 9th IFAC World Congress Budapest, Pergamon Press, 1984, pp. 243–247; H. Bock, Randwertproblemmethoden zur Parameteridentifizierung in Systemen nichtlinearer Differentialgleichungen, Dissertation, Bonner Mathematische Schriften, 1987, p. 183]. Numerical results show excellent performance for a benchmark enantiomer separation. Finally, the ability to solve the non-linear programs quickly also enables us to consider more challenging operating regimes like VARICOL [P. Adam, R. Nicoud, M. Bailly, O. Ludemann-Hombourger, Process and device for separation with variable-length chromatographic columns, US Patent 6,413,419 (2002)] and PowerFeed [Z. Zhang, M. Mazzotti, M. Morbidelli, PowerFeed operation of simulated moving bed units: changing flow-rates during the switching interval, J. Chromatogr. A 1006 (2003) 87–99].

Keywords: Simulated moving bed; VARICOL; PowerFeed; Multiple shooting; Non-linear optimization

Abbreviations: AE, algebraic equations; BDF, back differentiation formulas; CSS, cyclic steady state; DPF, dispersive plug flow model; gPROMS, general process modelling system; GC, gas chromatography; GRM, general rate model; HPLC, high performance liquid chromatography; ModiCon, SMB process with modulation of feed concentrations; MINLP, mixed integer non-linear problem; NLP, non-linear problem; PDE, partial differential equations; PowerFeed, SMB process mit variable flow rates; ODE, ordinary differential equations; SMB, simulated moving bed process; TMB, true moving bed process; VARICOL, variable column length process (asynchronous switching)

* Corresponding author. Tel.: +49 6221 54 88 31.
E-mail address: m.diehl@iwr.uni-heidelberg.de (M. Diehl).

0255-2701/$ – see front matter © 2007 Published by Elsevier B.V.
doi:10.1016/j.cep.2006.06.026

1. Introduction

Simulated moving bed (SMB) chromatography is gaining more and more attention. It is a mature separation technology applications of which are reported from different fields like biotechnological [11,4], pharmaceutical [12,13], petro-chemical [14] and food industry [15,16]. The SMB technology attracts interest particularly in the area of chiral separations [17,18], e.g. for pure drug development, where the resolution of enantiomers is usually a binary separation task with low selectivity and high operational costs. SMB processes are not only the method of choice for the purification of few grams of the chiral drug required by preliminary clinical tests but even more so for the large-scale production phase [18].

The optimization of SMB units has been widely studied by several research groups. The reported approaches can be grouped into two main categories. Optimization strategies within the first group make use of the true moving bed (TMB) model to approximate the SMB dynamics. The shortcut design method developed by the research group of Mazzotti and Morbidelli, called *triangle theory*, is one important representative [19,20]. It is widely employed by SMB practitioners due to its simplicity [21]. Two important characteristics are however not taken into account: the hybrid (non-steady) and non-linear nature of the SMB unit which may lead to sub-optimal or even infeasible operating points. In the second category, SMB models that account for column efficiency effects and the hybrid switching are used [22]. In this context, SMB models of different complexity are available [23]. Guiochon [24] reviewed these models in a recent publication and pointed out that they are predominantly simplifications of the rigorous general rate model (GRM) neglecting one or several physical effects. Gu [25] developed an efficient discretization strategy for the general rate model (GRM) that leads to simulation times of two orders of magnitude faster than real time. This is a pre-requisite for model-based optimization and control, and for an online optimization of SMB units that is attracting much interest recently [26–28].

Even with a numerically efficient general rate model, optimization of SMB processes requires a formidable numerical effort and it is still a challenging task. This is due to the fact that SMB processes do not reach a steady state but rather a periodic one. Furthermore, the periodic steady state is reached after several periods, the number of which depends mainly on the properties of the mixture and is not known a priori. One class of approaches that can be applied for the dynamic optimization of SMB processes are gradient-based numerical methods. In this context, a sequential or a simultaneous formulation can be used. In the first case, only the control variables are discretized. The dynamic system is decoupled from the optimization stage and is simulated using well-established techniques in order to evaluate the objective function and its constraints [29]. For the optimization of SMB processes this requires the computation of the cyclic steady state in each step of the optimizer. In the simultaneous or complete discretization approach the state variables and the controls are treated in the same fashion and the solution is carried out in the full space of variables [30]. This method results in a non-linear problem with a large number of variables and of non-linear equality constraints. The *direct multiple shooting method*, originally introduced by Bock [7], leads to a large, but specially structured NLP problem which is solved efficiently by a tailored SQP technique, taking advantage of the inherent problem structure. MUSCOD-II [31] is a recent implementation of the direct multiple shooting method that is able to treat general multi-stage control problems. It is used for the numerical investigations in this paper.

The remainder of this article is structured as follows: the Simulated Moving Bed principle is introduced in the next section. A rigorous process model is presented in Section 3. Section 4 discusses the SMB optimization problem and introduces the direct multiple shooting method in a general form. The application of the direct multiple shooting method is then reported in Section 5. Two different simultaneous implementations are discussed which differ in the way how they treat the cyclic steady state (CSS). Both simultaneous approaches are compared to each other and to the sequential approach in Section 6 where a validated non-linear enantio-separation model is considered as a case study. The availability of efficient numerical methods for the optimization enables to explore also the potential of more challenging operating regimes like VARICOL and PowerFeed which require a finer discretization of the operating parameters. Finally, a summary and some perspectives for future research are given.

2. Simulated moving bed processes

The chromatographic separation is based on the different adsorptivities of the components to a specific adsorbent which is fixed in a chromatographic column. The most simple process, batch chromatography, involves a single column which is charged with pulses of the feed solution. These feed injections are carried through the column by pure desorbent. While traveling through the column, the more adsorptive species is retained longer by the adsorbent thus leaving the column after the less adsorptive species. The separated peaks can be withdrawn as different fractions at the end of the column with the desired purity.

While the batch or elution chromatography mode has found the largest number of applications up to now, simulated moving bed (SMB) chromatography as a continuous process is gaining more and more attention due to its advantages in terms of productivity and eluent consumption [32,13]. In SMB chromatography, the adsorbent is distributed over a number of columns, 6 to 24 in standard applications [33]. Desorbent and feed streams enter the process continuously. A counter-current solid stream is approximated by shifting the inlet ports periodically in the direction of the internal recycle flow as shown in Fig. 1. Thus the solid stream is “simulated” by a discrete movement of columns rather than using a continuous stream. This leads to the desired separation of the feed components which can be withdrawn at the extract and raffinate ports which are shifted in the same manner as the inlets. In a case study, Nicoud and Majors [34] showed that the continuous SMB process reduces solvent consumption as much as 10-fold while using less column packing than batch chromatography.

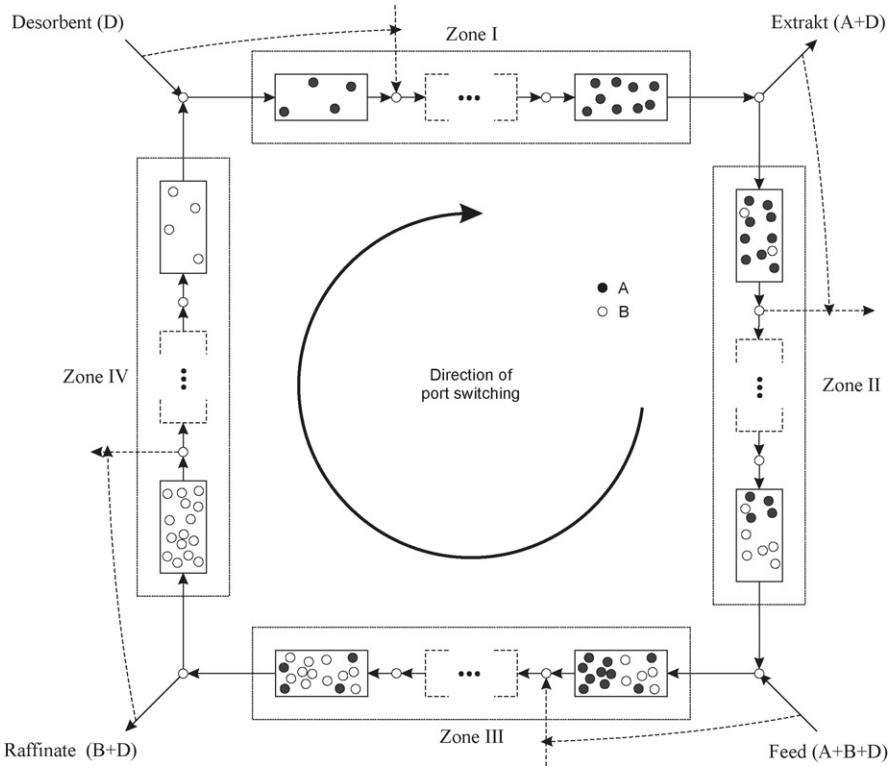

Fig. 1. Principle of the simulated moving bed process.

The classical SMB technology dates back to the 1960s and was invented by UOP for a petro-chemical application [33]. In the last decades, continuous development and improvement of the classical SMB scheme have led not only to a large number of new operating regimes, but also the in situ integration of reaction [35] or the application to supercritical and gaseous media have found increasing acceptance in research and practice [36–38]. Description of all SMB operating regimes is beyond the scope of this paper. We focus on three novel operating regimes which can be technically realized without a large modification of a classical SMB plant. Ludemann-Hombourger and Nicoud [39] proposed the so-called VARICOL process where an asynchronous shift of the inlet/outlet lines leads to a better allocation of the adsorbent and therefore to a higher productivity [40,29]. Zhang et al. [10] showed the potential of the variation of flow rates. This operating regime has been called PowerFeed and was optimized using a specially tailored genetic algorithm. In the ModiCon process, Schramm et al. [41], the feed solution is injected with variable concentrations using a gradient pump and obtained a significantly higher productivity for mixtures with highly non-linear adsorption.

Designing SMB processes involves, among other tasks, the selection of the number of columns per zone. A satisfactory operation is then achieved by proper selection of the flow rates (feed, desorbent, raffinate, extract and recycle) and of the switching times. Due to the discrete switching of the columns, SMB units do not reach a steady-state but rather a cyclic or periodic one. Fig. 2 shows the axial profiles along the columns at the beginning of a switching period for an optimized six-column SMB process. During each switching period, the concentration profiles "travel" through the columns and change their shape. When the cyclic steady state is reached, the concentration profiles at the end of a period are equal to those at the beginning of the period shifted by one column ahead in direction of the fluid flow. Assume that $\mathbf{f}_{\mathrm{smb}}$ represents the continuous dynamic of the SMB process during one switching period. The discrete shift by one column can be represented by a shifting matrix $\mathbf{P}$ which is listed in Appendix C. The continuous and the discrete dynamics can be collected into a mapping Γ:

$$\Gamma : \begin{cases} \underline{\mathbf{x}}^{k}_{\mathrm{smb}} = \mathbf{x}^{k}_{\mathrm{smb}} + \displaystyle\int_{t=0}^{\tau} \mathbf{f}_{\mathrm{smb}}(\mathbf{x}_{\mathrm{smb}}(t), \mathbf{u}_{\mathrm{smb}}(t), \mathbf{p})\,\mathrm{d}t, \\ \mathbf{x}^{k+1}_{\mathrm{smb}} = \mathbf{P}\underline{\mathbf{x}}^{k}_{\mathrm{smb}} \end{cases} \tag{1}$$

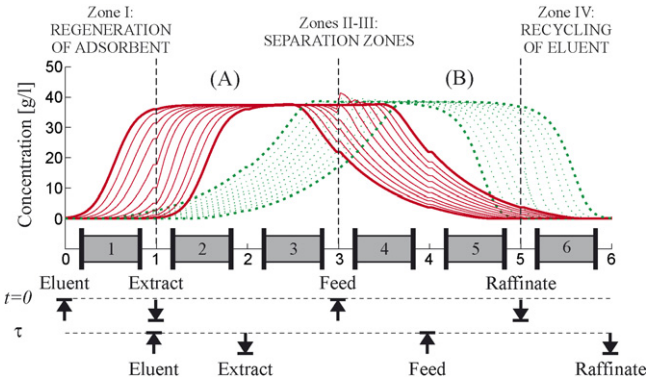

Fig. 2. Cyclic steady state.

where $\mathbf{x}_{\text{smb}}^{k}$ denotes the axial concentration profile along all columns at the beginning of the period k. The cyclic steady state (CSS) corresponds to

$$\mathbf{x}_{\text{smb}}^{k+1} = \Gamma(\mathbf{x}_{\text{smb}}^{k}) = \mathbf{x}_{\text{smb}}^{k} \tag{2}$$

τ denotes the period of the SMB process. $\mathbf{u}_{\text{smb}}$ is a vector of operating parameters such as the internal flow rates or the feed concentrations. $\mathbf{p}$ summarizes the physico-chemical parameters such as the isotherm constants or the mass transfer coefficients.

3. Dynamic process model

A rigorous mathematical first-principles model is used here in order to accurately calculate the concentration profiles $\mathbf{x}_{\text{smb}}$ in the chromatographic system. A lot of publications deal with modelling of chromatographic processes, e.g. Ganetsos et al. [42] and Gu [25]. Only some relevant aspects will be briefly discussed here. Accurate dynamic models of multi-column continuous chromatographic processes consist of dynamic models of each column and take into account the periodic port switching. From mass balances of the components around the inlet and the outlet nodes, the internal flow rates in the columns and the product concentrations (for components i = A, B) are calculated according to

$$\text{Desorbent node}: \quad Q_{\text{IV}} + Q_{\text{De}} = Q_{\text{I}} \tag{3}$$

$$c_{i,\text{IV}}^{\text{out}} Q_{\text{IV}} = c_{i,\text{I}}^{\text{in}} Q_{\text{I}} \tag{4}$$

$$\text{Extract node}: \quad Q_{\text{I}} - Q_{\text{Ex}} = Q_{\text{II}} \tag{5}$$

$$\text{Feed node}: \quad Q_{\text{II}} + Q_{\text{Fe}} = Q_{\text{III}} \tag{6}$$

$$c_{i,\text{II}}^{\text{out}} Q_{\text{II}} + c_{i,\text{Fe}} Q_{\text{Fe}} = c_{i,\text{III}}^{\text{in}} Q_{\text{III}} \tag{7}$$

$$\text{Raffinate node}: \quad Q_{\text{Ra}} + Q_{\text{IV}} = Q_{\text{III}} \tag{8}$$

Here $Q_{\text{I–IV}}$ denote the flow rates in the corresponding zones, Q_{De}, Q_{Ex}, and Q_{Fe} are the external flow rates, and $c_{i,z}^{\text{out}}$ and $c_{i,z}^{\text{in}}$ denote the concentrations of component i in the stream leaving or entering the respective zone z.

Guichon [24] in a recent article reviewed different modelling approaches and pointed out that all of them can be derived from the general rate model (GRM) of chromatography which accounts for the following effects in a chromatographic column (see Fig. 3):

- convection,
- axial dispersion,
- pore diffusion,
- mass transfer between the liquid and the solid phase,
- multi-component adsorption.

We assume that the solid phase consists of porous, uniform and spherical particles (radius R_{p}, radial coordinate r) with void fraction ε_{p}, and that a local equilibrium is established within the pores. The concentration of component i is denoted by $c_{\text{b},i}$ in the fluid phase and by q_i in the solid phase. ε_{b} is the void fraction of the bulk phase, D_{ax} the axial dispersion coefficient, c_i^{eq}

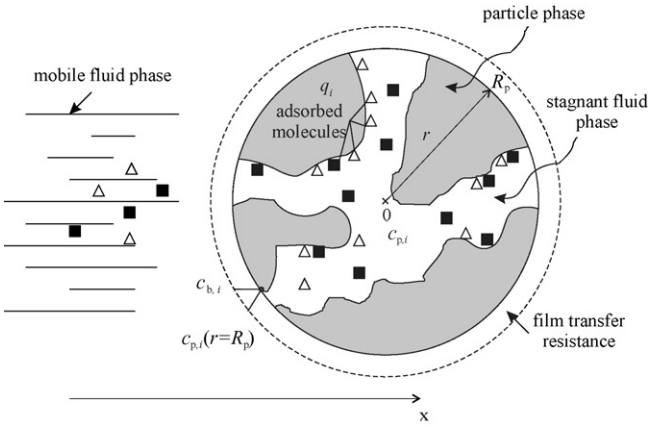

Fig. 3. General rate model.

the equilibrium concentration, $k_{\text{l},i}$ the film mass transfer resistance coefficient, and $D_{\text{p},i}$ the diffusion coefficient within the particle pores. The concentration within the pore is denoted by $c_{\text{p},i}$. The following set of partial differential equations can be derived from a mass balance around an infinitely small cross-section area of the column, if constant radial distribution of the interstitial velocity u and the concentrations c_i is assumed:

$$\frac{\partial c_{\text{b},i}}{\partial t} + \frac{(1-\varepsilon_{\text{b}})3\,k_{\text{l},i}}{\varepsilon_{\text{b}} R_{\text{p}}}(c_{\text{b},i} - c_{\text{p},i}|_{r=R_{\text{p}}}) = D_{\text{ax}}\frac{\partial^2 c_{\text{b},i}}{\partial x^2} + u\frac{\partial c_{\text{b},i}}{\partial x} \tag{9}$$

$$(1-\varepsilon_{\text{p}})\frac{\partial q_i}{\partial t} + \varepsilon_{\text{p}}\frac{\partial c_{\text{p},i}}{\partial t} - \varepsilon_{\text{p}} D_{\text{p},i}\left[\frac{1}{r^2}\frac{\partial}{\partial r}\left(r^2\frac{\partial c_{\text{p},i}}{\partial r}\right)\right] = 0 \tag{10}$$

with initial and boundary conditions

$$c_{\text{b},i}|_{t=0} = c_{\text{b},i}(t=0,x), \quad c_{\text{p},i}|_{t=0} = c_{\text{p},i}(t=0,x,r) \tag{11}$$

$$\left.\frac{\partial c_{\text{b},i}}{\partial x}\right|_{x=0} = \frac{u}{D_{\text{ax}}}(c_{\text{b},i} - c_i^{\text{in}}), \quad \left.\frac{\partial c_{\text{b},i}}{\partial x}\right|_{x=L} = 0 \tag{12}$$

$$\left.\frac{\partial c_{\text{p},i}}{\partial r}\right|_{r=0} = 0, \quad \left.\frac{\partial c_{\text{p},i}}{\partial r}\right|_{r=R_{\text{p}}} = \frac{k_{\text{l},i}}{\varepsilon_p D_{\text{p},i}}(c_{\text{b},i} - c_{\text{p},i}|_{r=R_{\text{p}}}) \tag{13}$$

From a mathematical point of view, it is useful to distinguish chromatographic processes by the type of adsorption isotherms $q_i(c_{\text{p},i})$. Processes with linear or simple Langmuir isotherms lead to systems of uncoupled partial differential equations which are easier to solve than those with coupled non-linear adsorption behavior, e.g. competitive Langmuir isotherm:

$$q_i = \frac{H_i c_{\text{p},i}}{1 + \sum_{j=1}^{n_{\text{sp}}} k_j\, c_{\text{p},j}}, \quad i = 1,\ldots,n_{\text{sp}} \tag{14}$$

with H_i and k_i as isotherm constants. n_{sp} denotes the number of species involved in the separation.

3.1. PDE discretization

The resulting system of coupled partial differential equations (9) and (10) can be solved efficiently by using the numerical

approach proposed in Gu [25] where a Galerkin finite element discretization (of order two) of the bulk phase is combined with an orthogonal collocation of the solid phase. This numerical method was first applied to SMB processes by Dünnebier et al. [22]. It is considerably more efficient than classical finite differences discretization methods. The bulk phase is divided into n_{fe} quadratic finite elements and the solid phase is discretized using n_c collocation points. As a result, the partial differential equations (PDE) are transformed into an ordinary differential equations system (ODE) of the following form:

$$\dot{\mathbf{x}}_{col}(t) = \mathbf{f}_{col}(\mathbf{x}_{col}(t), \mathbf{u}_{col}(t), \mathbf{p}, t), \quad \mathbf{x}_{col}(0) = \mathbf{x}_{col,0},$$
$$\mathbf{c}_{out}(t) = \mathbf{h}_{col}(\mathbf{x}_{col}(t)) \tag{15}$$

with the differential variables $\mathbf{x}_{col}(t) \in \mathbb{R}^{neq_{col}}$, the inputs $\mathbf{u}_{col}(t) \in \mathbb{R}^{n_u}$, the parameters $\mathbf{p} \in \mathbb{R}^{n_p}$ and the outputs $\mathbf{c}_{out}(t) \in \mathbb{R}^{n_{sp}}$. The state vector $\mathbf{x}_{col}(t) \in \mathbb{R}^{neq_{col}}$ includes the concentrations in the liquid and in the solid phases at the grid nodes and has the dimension:

$$neq_{col} = n_{sp}(n_c + 1)(2\,n_{fe} + 1) \tag{16}$$

The input vector $\mathbf{u}_{col} \in \mathbb{R}^{n_u}$ consists of the internal flow rate and the concentrations at the inlet of the column:

$$\mathbf{u}_{col}(t) = [Q_{col}(t), \mathbf{c}_{in}(t)]^T, \quad n_u = n_{sp} + 1 \tag{17}$$

$\mathbf{p} \in \mathbb{R}^{n_p}$ summarizes all parameters, e.g. isotherm constants, mass transfer coefficients etc.. Finally, $\mathbf{c}_{out} \in \mathbb{R}^{n_{sp}}$ describes the concentrations at the outlet of the column which are equal to the fluid phase concentrations at the last finite element node.

The ODE-system (15) is large which is typical for distributed systems described by partial differential equations, e.g. for $n_{fe} = 12$, $n_c = 1$ the dynamic model of a single chromatographic includes 100 state variables. The resulting ODE-system is also stiff due to large differences in the dynamics of the interacting effects as, e.g. convection and diffusion. Using the implicit integrator LSODI which is based on the backwards differentiation formulas (BDF) [43] and suitable for stiff problems, the process model can be integrated about five orders of magnitude faster than real time. The Jacobian of the model equations has a width of eight elements around the diagonal due to the specially structured spatial discretization [25]. This is exploited by LSODI what reduces the calculation time significantly.

3.2. Multi-stage simulated moving bed processes

As already mentioned, the SMB loop connects the single chromatographic columns while satisfying the node restrictions (3)–(8). The state vector $\mathbf{x}_{smb} \in \mathbb{R}^{neq_{smb}}$ is composed of the single column vectors:

$$\mathbf{x_{smb}} = [\mathbf{x}_{col}^1, \mathbf{x}_{col}^2, \ldots, \mathbf{x}_{col}^{n_{col}}]^T, \qquad neq_{smb} = n_{col} neq_{col} \tag{18}$$

where n_{col} denotes the number of columns. The input vector $\mathbf{u}_{smb}$ is built similarly. However, due to the node conditions (3)–(8), the column inputs are not independent from each other. The degrees of freedom are reduced to the flow rates of desorbent, extract, feed and recycle $\mathbf{u}_{smb} = [Q_{De}, Q_{Ex}, Q_{Fe}, Q_{Re}]^T$. The raffinate flow rate then results from the overall mass balance. Thus, the SMB process is described by the following large-scale ODE-system when the single column dynamics are augmented to $\mathbf{f}_{smb} = [\mathbf{f}_{col}^1, \ldots, \mathbf{f}_{col}^{n_{col}}]^T$:

$$\dot{\mathbf{x}}_{smb}(t) = \mathbf{f}_{smb}(\mathbf{x}_{smb}(t), \mathbf{u}_{smb}(t), \mathbf{p}, t), \qquad \mathbf{x}_{smb}(0) = \mathbf{x}_{smb}, 0 \tag{19}$$

The new operating regime VARICOL consists of asynchronous switching of the inlet/outlet positions. In the PowerFeed process the flow rates vary with time. Both processes can be considered as a multi-stage SMB process as indicated in Fig. 4. Hereby, the switching period τ is divided into a number of stages n_{stages} with durations δt_i. The stages are simulated successively and equality constraints are imposed between the stages. The operating conditions, i.e. the flow rates or the positions of the inlet/outlet ports, may change from stage to stage.

4. Problem overview

Optimal operation of SMB processes requires to determine the optimal operating parameters with respect to an economical objective function. For this purpose, a single-objective optimization problem is formulated for a multi-stage SMB process $i = 1, \ldots, n_{stages}$:

$$\begin{aligned} \min_{Q_{De}^i(t), Q_{Fe}^i(t), Q_{Ra}^i(t), Q_{Re}^i(t), \delta t_i, \tau, \mathbf{x}_{smb}} \quad & Cost_{spec} \\ \text{subject to (s.t.)} \quad & \Gamma(\mathbf{x}_{smb}(\tau)) - \mathbf{x}_{smb}(0) = 0, \\ & Pur_{Ex} \geq Pur_{Ex,\,min}, \\ & Pur_{Ra} \geq Pur_{Ra,\,min}, \\ & 0 \leq \mathbf{x}_{smb}, \\ & 0 \leq \tau, \\ & 0 \leq Q_{col}^{ij} \leq Q_{max}, \quad j = 1, \ldots, n_{col} \end{aligned} \tag{20}$$

The aim is to find a cyclic steady state (CSS) with operating conditions that lead to minimal separation costs $Cost_{spec}$ while satisfying the purity requirements and plant restrictions. An additional constraint takes the maximal allowable pressure drop into account. The main difficulty of the optimization problem (20) comes from the large dimension of the cyclic steady state equations when a rigorous first-principles plant model is used [44], e.g. for an eight-column SMB process 800 state variables have to be considered. Moreover, SMB processes exhibit a strongly non-linear behavior due to competitive multicomponent adsorption and the interplay between continuous and hybrid dynamics. Only model-based approaches can exploit the full optimization potential and deal with the large number of optimization variables. Another advantage of model-based approaches is the simple inclusion of further design parameters as, e.g. the column length or the column diameter. Logical or integer-valued design parameters, e.g. the number of columns, however, lead to complex mixed integer non-linear problems (MINLP) which will not be discussed here.

Eq. (20) comprises a complex dynamic optimization problem the solution of which essentially depends on an efficient and reliable computation of the cyclic steady state. Two main approaches can be distinguished:

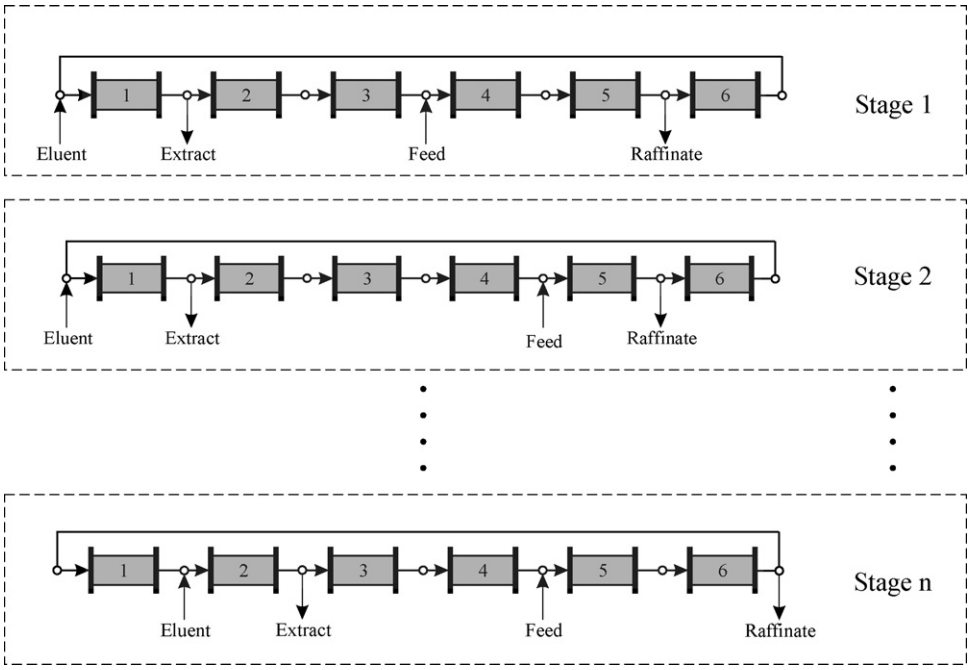

Fig. 4. The VARICOL process modelled as a multi-stage SMB process.

(I) *Sequential direct dynamic simulation*. Here a dynamic simulation of the process is performed until the cyclic steady state is reached, which is equivalent to a repeated evaluation of Eq. (2). The advantage of this approach is its robustness and simplicity, which is based on the fact that there is no need for any other numerical techniques besides the solution of a system of differential equations. The sequential or black-box approach is capable of dealing with very detailed and complicated models. It is, therefore, widely used in both industry and academia. The disadvantages are that only stable cycles can be found, that there are no a priori estimates on the convergence behavior, that at best linear convergence can be achieved [45], and that the convergence is determined by the properties of the system and cannot be controlled. The software package SMBOPT is based on this concept. The VARICOL operating regime was treated by this technique as well [29,44].

(II) *Simultaneous approach*. In the simultaneous approach, both the controls and the related state trajectory are determined in the optimization loop. The periodicity condition (CSS) is formulated as an additional constraint of the optimization problem. Two types of simultaneous methods have been proposed in the literature [30,46]. In the full discretization approach [45,30], the dynamic state equations are further discretized with respect to time and the cyclic steady state is reduced to a set of non-linear algebraic equations (AE). The second method is a multiple shooting method [47,46]. Here, a switching period is divided into several sub-intervals. The differential equations are integrated over time along with parallel sensitivity information for the solutions with respect to control and state variables. The sensitivities are then returned to a specially tailored SQP solver which determines a new guess for both the state and the control variables (see Fig. 5). In both cases, a large optimization problem results and special numerical methods are required. The main advantages of simultaneous approaches in conjugation with quasi-Newton methods is that theoretically they attain super-linear convergence near the solution [45]. Another advantage is that the cyclic steady state has to be reached only at the optimum, the time-consuming CSS convergence loop is eliminated. However, such approaches can still be prohibitively expensive in the simulated moving bed context given the size and the computational effort.

Kloppenburg [48] applied a full-discretization approach to the optimization of SMB processes. The model was discretized with respect to time using a trapezoidal rule. Two alternatives methods were used for the solution of the resulting non-linear algebraic equalities (AE): (1) formulation of the dynamic model equations using DIVA [49] as a code generator, temporal discretization and solution with the non-linear equation solver NLEQIS [50], and (2) formulation of the model in the modelling language AMPL [51] and solution with the large-scale

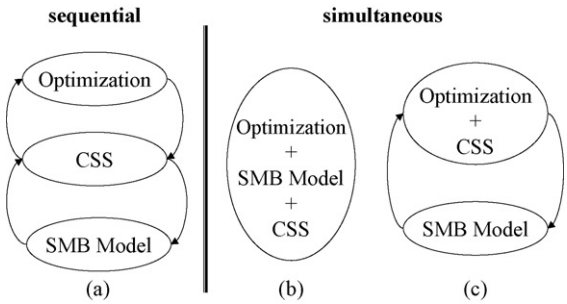

Fig. 5. (a) Sequential approach, (b) full discretization and (c) multiple shooting.

solver LANCELOT [52]. The second approach was faster since LANCELOT is specially designed for large-scale sparse nonlinear equations. In Kloppenburg and Gilles [53] also the gain of flow rates modulation was pointed out. However, bad convergence and robustness of the numerical methods limited the number of time-intervals and prevented the full exploitation of the PowerFeed process [48].

In a recent publication, Minceva et al. [54] re-implemented Kloppenburg's [48] full discretization method with the aim to accelerate the CSS simulation of a simulated moving bed process for an enantiomer-separation. They developed two simulation models in the general process modelling system (gPROMS) using a transport dispersive model (DPF) which is usually sufficiently accurate. In the first model, they imposed the periodicity over a whole cycle, a cycle being a period multiplied by the number of columns. In the second one, they formulated Eq. (2) as an additional equality constraint. The obtained results were encouraging since the second simulation model required less computation time than the successive method while maintaining a high accuracy. A high-resolution second-order backward difference method (BFDM) was used for spatial and for temporal discretization. The selection of an appropriate discretization method seems to be essential and can be the reason why Kloppenburg's [48] method failed. Coarse discretization introduces physically unrealistic numerical oscillations near steep adsorption fronts [55]. However, in the reported case study, Minceva et al. [54] used only three finite elements, which was sufficiently accurate for the operating conditions considered there. But they also pointed out that for steep profiles, e.g. for systems with fast mass transfer, finer grids should be used. In this case, as shown by the first simulation model, an eight-fold increase of the dimension leads to a computational effort two orders of magnitude higher than for the sequential approach [54].

The full discretization method has the main drawback that no control over the temporal discretization error exists. Therefore a high-resolution grid for the temporal discretization is required what enlarges the dimension of the resulting AE-problem. Work in the field of pressure swing adsorption (PSA) optimization over the last 20 years have clearly shown that the full-discretization method is suitable for rather simple and small adsorption models [47]. PSA are periodic processes with some similarities to SMB processes.

The multiple shooting method overcomes the problem of the temporal discretization error since fully adaptive DAE solver can be employed. In this article we propose an efficient, flexible and reliable optimization strategy based on the multiple shooting method. It incorporates realistic, detailed process models and rigorous solution procedures. The optimization problem (20) is formulated as a multi-stage optimal control problem allowing to include more complex operating regimes like VARICOL and PowerFeed. To our knowledge, this is the first efficient implementation of this numerical technique to the SMB process and its related operating regimes. In the next section, we introduce a general multi-stage optimal control problem to which the multiple shooting method implemented in the software package MUSCOD-II can be applied. Section 5 then presents two different ways for the formulation of the SMB problem (20).

4.1. Formulation of multi-stage optimal control problems in MUSCOD-II

Many dynamic process optimization problems can be expressed as multi-stage optimal control problems for DAE. The time horizon of interest $[t_0, t_M]$ is divided into M subintervals, i.e. M corresponds to the number of stages n_{stages} in case of multi-stage SMB processes. The aim is to minimize a generalised Mayer-type objective function which is the sum of pointwise defined scalar functions ϕ_i.

$$\min_{x_i, z_i, u_i, p, t_i} \sum_{i=0}^{M-1} \phi_i(x_i(t_{i+1}), z_i(t_{i+1}), p, t_{i+1}) \tag{21}$$

subject to the model stages $i = 0, 1, \ldots, M-1$ modelled by DAE:

$$\dot{x}_i(t) = f_i(x_i, z_i, u_i, p, t), \qquad 0 = g_i(x_i, z_i, u_i, p, t),$$
$$t \in [t_i, t_{i+1}] \tag{22}$$

the control and path constraints $i = 0, 1, \ldots, M-1$:

$$h_i(x_i, z_i, u_i, p, t) \geq 0, \quad t \in [t_i, t_{i+1}] \tag{23}$$

the stage transition conditions $i = 0, 1, \ldots, M-2$:

$$x_{i+1}(t_{i+1}) = c_i(x_i(t_{i+1}), z_i(t_{i+1}), p) \tag{24}$$

and the multipoint boundary conditions:

$$\sum_{i=0}^{M-1} [r_i^s(x_i(t_i), z_i(t_i), pt_i) + r_i^e(x_i(t_{i+1}), \ldots)] \left\{ \begin{matrix} = \\ \geq \end{matrix} \right\} 0 \tag{25}$$

The control vector on stage i is denoted by $u_i(t)$, the differential and algebraic states by $x_i(t)$ and $z_i(t)$ ($t \in [t_i, t_{i+1}]$). The vector p contains global model parameters. The dynamic model equations and also their number may change from one stage to the next; the coupling is provided by the stage transition conditions (24). Continuous control and path constraints (23) and general, linearly coupled multipoint boundary conditions (25) are included.

This type of problems can be solved efficiently with the software package MUSCOD-II [6,31,56]. The optimization variables u_i are approximated by a *piecewise* representation. This is done by first dividing each model stage into a number of subintervals called multiple shooting intervals as indicated in Fig. 6. Additional optimization variables s_{ij}^x, s_{ij}^z are added as initial values for the differential and algebraic variables. The infinite dimensional optimization problem is transformed into a non-linear program (NLP) which is then solved by a specially designed sequential quadratic programming (SQP) algorithm [6]. The basic concept of the direct multiple shooting method is to solve the differential (algebraic) equations *independently* on each of the multiple intervals. Consistency of the algebraic equations and, particularly, continuity of the state trajectory at the multiple shooting grid points are incorporated as constraints into the NLP. They are satisfied only at the solution of the problem, but not necessarily during the SQP iterations. This allows to easily incorporate information about the expected trajectory

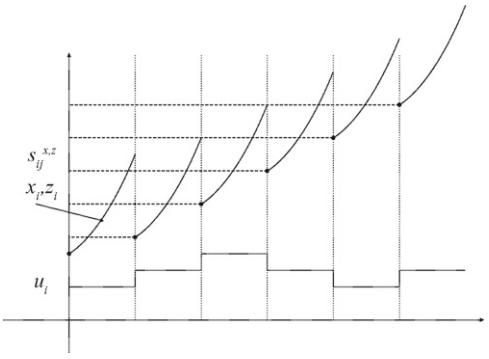

Fig. 6. Control and state parameterization by multiple shooting.

into the initial guess, and it leads to good convergence properties. For more details, see e.g. [57,6].

The efficiency of the approach, which has been observed in many practical applications, has several reasons. One of the most important is the inclusion of information about the behavior of the state trajectory (which is often well-known) into the initial guess for the iterative solution procedure; this can dampen the influence of poor initial guesses for the optimization variables (which are usually much less known). Multiple shooting has been shown to be considerably more stable and efficient than single shooting for the solution of boundary value problems.

MUSCOD-II provides interfaces to FORTRAN, C, gPROMS and SIMULINK in order to formulate the dynamic optimization problem [56]. Subroutines have to be specified for the stages, transition stages, constraints and objective function.

5. Optimization strategies for the SMB process

In this article, we distinguish three different optimization strategies:

- *The sequential method*: the cyclic steady state is reached by successive simulation in each step of the optimization. The optimization involves only the operating parameters. It is described in more detail in [58].
- *The "exact" multiple shooting method*: it consists of the standard implementation of the optimization problem (20) in MUSCOD-II. Thus, the cyclic steady state is formulated as an additional equality constraint of a multi-stage optimal control problem.
- *The "approximated" multiple shooting method*: hereby the optimization problem is formulated at the cyclic steady state. Additional relationships are imposed to the inlet/outlet concentrations and to the flow rates of the different chromatographic column to enforce a multi-stages SMB process. The inlet/outlet concentrations are time-dependent functions. They are parameterized using Legendre polynomials leading to a finite dimensional NLP problem.

In the following sections, if not said explicitly, the "exact" method will be referred to as Method I and the "approximated" method as Method II.

5.1. Sequential approach

As already indicated in Fig. 5, in the sequential approach two loops have to be distinguished. In an inner loop, the model is simulated until the cyclic steady state is reached. At the cyclic steady state the objective function and the constraints formulated in the optimization problem (20) are evaluated and given back to a non-linear optimizer. The resulting optimization problem, in the outer loop, is small and can be solved using any non-linear optimization routine. The feasible path SQP solver FFSQP [59] showed the best robustness and convergence properties in the presence of highly non-linear purity constraints [29].

The simulation of the process model can be accelerated by one order of magnitude when the SMB loop is opened at the recycle point, the point located between zones I and IV. The concentration profile at the outlet of zone IV saved during the last period is used to evaluate the first column in zone I. Afterwards the SMB loop is simulated sequentially column by column and the scheme is repeated until cyclic steady state is reached. The first column does not influence the last column much due to a large spatial distance between both columns. A high dilution of the inlet of the first column contributes even more to this decoupling. Additionally, in the neighborhood of the optimum the recycle stream (here defined as the stream between zones I and IV) is mostly pure. Otherwise a decontamination of the extract port results which has to be avoided by the optimizer.

Todd et al. [60] proposed a node refinement method to accelerate the successive substitution until CSS. The simulator commences with the small number of internal node points and runs until the CSS is achieved. The low number of nodes results in a reduced calculation time. Then using cubic-spline interpolation, the CSS is mapped to a finer level of discretization and the obtained profile is simulated with more internal node points until the CSS is reached. This process is repeated as many times as necessary until no changes from one node refinement to the next occur. Todd et al. [60] have reduced the computational time by a factor two. However, this approach cannot be applied to the discretization scheme used here because it is non-conservative. By a coarse discretization, physically unrealistic and even negative concentrations occur near sharp fronts. Moreover the SMB process reaches a cyclic steady state after 100–400 periods which is much faster than the PSA process investigated by Todd et al. [60] where slow convectively driven thermal waves are moving through the system and usually more than 1000 periods are required.

The optimizer additionally requires the gradients of the objective functions and of the constraints with respect to the optimization variables. They are calculated using a forward finite difference scheme which re-simulates the model with perturbed optimization variables. Since the CSS-evaluation is the most time-consuming computation, the numerical effort needed for the whole optimization procedure increases linearly with respect to the number of optimization variables.

The successive simulation corresponds to the evaluation of Γ for a number of cycles n_{css} until the cyclic steady state (CSS)

is reached:

$$\mathbf{x}_{\mathrm{smb}}^{\mathrm{css}} = \underbrace{\Gamma(\Gamma(\Gamma\cdots(\Gamma}_{n_{\mathrm{css}}}(\mathbf{x}_{\mathrm{smb}}^{0})))) \tag{26}$$

$\mathbf{x}_{\mathrm{smb}}^{0}$ is initialized by zero, thus commencing the simulation with columns containing pure solvent. In some cases, the convergence to the CSS is faster when the computation is initialized from a previously calculated CSS. However, the number of cycles n_{css} is not known a priori. That is the reason why the difference of the profiles between two successive periods is checked numerically using the two-norm:

$$\|\mathbf{x}_{\mathrm{smb}}^{\mathrm{css}} - \Gamma(\mathbf{x}_{\mathrm{smb}}^{\mathrm{css}})\|_2 \leq \varepsilon_{\mathrm{css}} \tag{27}$$

In addition to Eq. (27), the overall mass balance is checked numerically to ensure the accuracy of the spatial discretization. If $m_{\mathrm{in,out}}$ are the masses entering and leaving the SMB process during a period of time, then the following relationship must hold:

$$100 \times \frac{m_{\mathrm{in}} - m_{\mathrm{out}}}{m_{\mathrm{in}}} \leq m_{\mathrm{css}} \tag{28}$$

where m_{css} denotes the maximum allowed mass balance mismatch in percent. Eq. (28) is usually not fulfilled by a coarse spatial discretization. In such cases, the remedy is to increase the number of nodes.

5.2. Method I

The implementation of Method I in MUSCOD-II is straightforward, once an interface to the dynamic process model is available. The general rate model is completely implemented in the programming language FORTRAN [29] and has been integrated in the software package MUSCOD-II.

5.2.1. Stages and transition stages

A stage consists of one SMB loop with given positions of the inlet/outlet lines. Continuity constraints are imposed between the stages as shown in Fig. 4. By definition, the desorbent line is always positioned before column number one. Assume that p, q are the respective positions of the extract and raffinate lines. Then the following ODE-system is formulated for each stage k:

$$\dot{\mathbf{x}}_{\mathrm{smb}} = \mathbf{f}_{\mathrm{smb}}(\mathbf{x}_{\mathrm{smb}}(t), \mathbf{u}_{\mathrm{smb}}(t), \mathbf{p}, t), \qquad \dot{\mathbf{m}}_{\mathrm{Ex}} = \mathbf{c}_{\mathrm{out}}^{p} Q_{\mathrm{Ex}},$$
$$\dot{\mathbf{m}}_{\mathrm{Fe}} = \mathbf{c}_{\mathrm{Fe}} Q_{\mathrm{Fe}}, \qquad \dot{\mathbf{m}}_{\mathrm{Ra}} = \mathbf{c}_{\mathrm{out}}^{q} Q_{\mathrm{Ra}}, \quad t \in [0, \delta t_k] \tag{29}$$

The differential states variables $\mathbf{m}_{\mathrm{Ex}}, \mathbf{m}_{\mathrm{Fe}}, \mathbf{m}_{\mathrm{Ra}}$ represent the integral mass entering or leaving the respective ports for the different components during one switching period. As shown in Table 1, they enable an easier evaluation of the performance measures needed in the optimization problem (20).

5.2.2. Constraints

The cyclic steady is formulated as a multipoint boundary condition (25) with:

$$\mathbf{r}_0^{\mathrm{s}} = \mathbf{x}_{\mathrm{smb}}(t = 0) \tag{30}$$

Table 1
Definition of process performance parameters

Performance parameter	Extract	Raffinate
Purity (%)	$100 \times \frac{m_{\mathrm{Ex}}(1)}{m_{\mathrm{Ex}}(1) + m_{\mathrm{Ex}}(2)}$	$100 \times \frac{m_{\mathrm{Ra}}(2)}{m_{\mathrm{Ra}}(1) + m_{\mathrm{Ra}}(2)}$
Recovery (%)	$100 \times \frac{m_{\mathrm{Ex}}(1)}{m_{\mathrm{Fe}}(1)}$	$100 \times \frac{m_{\mathrm{Ra}}(2)}{m_{\mathrm{Fe}}(2)}$
Productivity (g/h)	$\mathrm{Pr}_{\mathrm{Ex}} = \frac{m_{\mathrm{Fe}}(1)}{\tau}$	$\mathrm{Pr}_{\mathrm{Ra}} = \frac{m_{\mathrm{Fe}}(2)}{\tau}$

$\mathrm{Pr} = \mathrm{Pr}_{\mathrm{Ex}} + \mathrm{Pr}_{\mathrm{Ra}}$.

$$\mathbf{r}_{(n_{\mathrm{stages}}-1)}^{\mathrm{e}} = -\mathbf{P}\mathbf{x}_{\mathrm{smb}}(t = \tau) \tag{31}$$

It has to be remarked that the stages are enumerated in MUSCOD-II starting with zero. As stated in Eq. (25), MUSCOD-II ensures that $\sum r_i^{\mathrm{s}} + r_i^{\mathrm{e}} = 0$. This is equivalent to requiring a cyclic steady state since the states at the beginning of the period are then equal to those at the end, shifted back by one column.

5.3. Method II

Here, each single chromatographic column is considered as a stage. The main idea behind this method is to formulate the optimization problem such that a large part of the cyclic steady state condition is fulfilled directly. At the cyclic steady state, the axial profile of a given column at the end of the period is equal to that of the previous column, but at the start of the period (see Fig. 7):

$$\mathbf{x}_{\mathrm{col}}^{i}(t = \tau) = \mathbf{x}_{\mathrm{col}}^{i-1}(t = 0) \tag{32}$$

If the stages are ordered in the opposite way than the columns as illustrated in Fig. 7, condition (32) is fulfilled directly by imposing a continuity constraint between the stages j and $j + 1$. However, the stages are further coupled by the inlet/outlet concentrations and the flow rates between the columns. We propose to approximate the inlet/outlet concentrations by Legendre polynomials and to impose additional relationships on them.

Methods I and II differ in the way they consider the periodicity conditions. Consider a four-column SMB process as illustrated

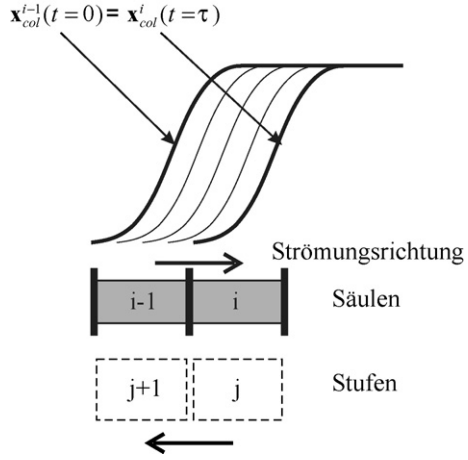

Fig. 7. Illustration of Method II.

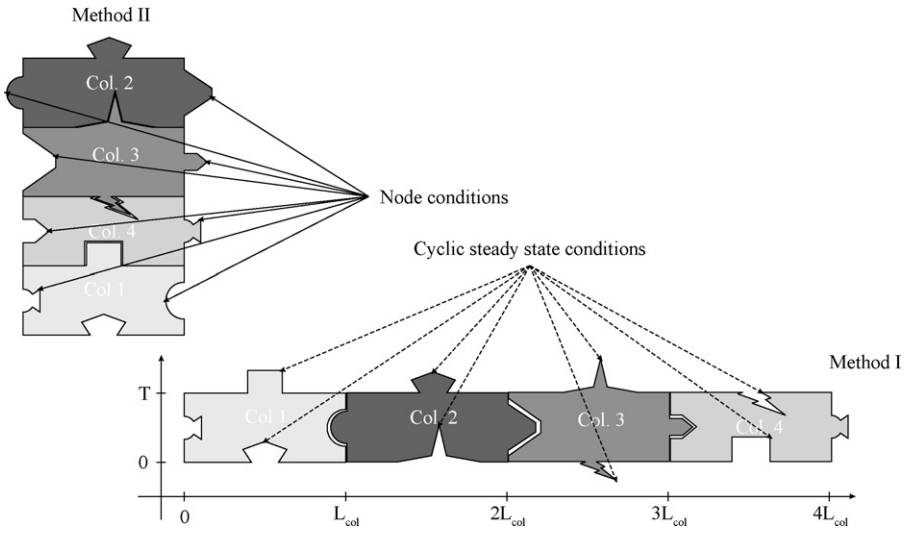

Fig. 8. Illustration of Methods I and II.

in Fig. 8. The horizontal arrangement corresponds to Method I. The columns are connected to build a SMB ring. The node conditions are fulfilled internally as indicated by the matching left/right sides of the columns. The cyclic steady state conditions couple the concentration profiles at the start and at the end of the period. This is indicated by the matching upper/lower sides, e.g. the concentration profile at the beginning of the period over the first column (lower side) is equal to the concentration profile at the end of the period over column 2 (upper side). Method II rearranges the two-dimensional domain in time and space, as shown in the vertical arrangement in Fig. 8. As a result, the cyclic steady state is now fulfilled internally. On the other hand, the node conditions are imposed as additional equality constraints. Thus the SMB optimization problem has an analogy to a puzzle which can be put together into two different ways.

It has to be noted that this approach differs from a low-order parameterization of the cyclic steady state where the axial profile $\mathbf{x}_{smb}$ itself is approximated by polynomials, splines, Fourier transformation, or eigenfunction expansion. In our approach, convergence to CSS is ensured since the Legendre approximation between the columns can be seen as additional non-linear "virtual" plant components which smooth the outlet signals to the next "best" Legendre polynomials. Low-dimensional parameterization of the cyclic steady state may lead to infeasibility and a special numerical treatment of the error introduced by the low-parameterization itself is required [47].

The main advantage of Method II is that the number of differential equations is reduced in the optimization problem. However, a multi-stage SMB process, e.g. VARICOL or PowerFeed, requires an additional synchronization effort. Fig. 9 shows such a multi-stage SMB process that is subdivided into n_{int} sub-intervals. In each sub-interval, each single chromatographic column of the SMB loop is represented by its own stage. All stages ordered below a given column describe the behavior of that column over time, whereas all stages ordered horizontally are coupled together by an SMB loop describing one of the sub-intervals of the SMB process. Thus the horizontal arrows denote relationships between the columns in terms of inlet/outlet concentrations and flow rates. The vertical arrows show the order of the stages in MUSCOD-II.

As shown in Fig. 9, the time period τ is discretized into n_{int} intervals which are not necessarily equidistant. The total number of stages results as

$$n_{stages} = n_{col} n_{int} \tag{33}$$

5.3.1. Stages and transition stages

Between the stages simple continuity conditions are imposed. Apart from the coupling between the last and the first column, the cyclic steady state condition is directly imposed by continuity conditions between the stages. Fig. 10 summarizes the inputs and outputs of a single chromatographic column. The following DAE-system is formulated for each stage k with $n_s = 1, \ldots, n_{sp}$:

$$\dot{\mathbf{x}}_{col} = \delta t_k \mathbf{f}_{col}(\mathbf{x}_{col}(t), \mathbf{u}_{col}(t), \mathbf{p}, t), \qquad \dot{\mathbf{m}}_{Ex} = \mathbf{c}_{out} Q_{Ex},$$
$$\dot{\mathbf{m}}_{Fe} = \mathbf{c}_{Fe} Q_{Fe}, \qquad \dot{\mathbf{m}}_{Ra} = \mathbf{c}_{out} Q_{Ex},$$
$$\dot{\mathbf{q}}_{out,1} = c_{out,1}(t)\,\Phi(t), \ldots, \dot{\mathbf{q}}_{out,n_{sp}} = c_{out,n_{sp}}(t)\,\Phi(t),$$
$$0 = c_{in,1}(t) - \mathbf{q}_{in,1}^{T}\,\Phi(t), \ldots, 0 = c_{in,n_s}(t) - \mathbf{q}_{in,n_s}^{T}\,\Phi(t),$$
$$t \in [0, 1] \tag{34}$$

For each stage k the following extended input and state vectors are defined:

$$\mathbf{x}^k = [\mathbf{x}_{col}^k, \mathbf{m}_{Ex}^k, \mathbf{m}_{Fe}^k, \mathbf{m}_{Ra}^k, \mathbf{q}_{out}^k, \Delta\mathbf{c}_{out}^k]^T \tag{35}$$

$$\mathbf{u}^k = [Q_{De}^k, Q_{Ex}^k, Q_{Fe}^k, Q_{Ra}^k, Q_{int}^k, \mathbf{q}_{in}^k]^T \tag{36}$$

The time evolution of the vector $\mathbf{x}_{col}$ describes the dynamics of the chromatographic column according to Eq. (15). $\mathbf{m}_{Ex}$, $\mathbf{m}_{Fe}$, $\mathbf{m}_{Ra}$ denote the integral mass leaving or entering the respective ports during one switching period. The vectors $\mathbf{q}_{in}$ and $\mathbf{q}_{out}$ represent the Legendre approximation of the inlet and outlet concentrations.

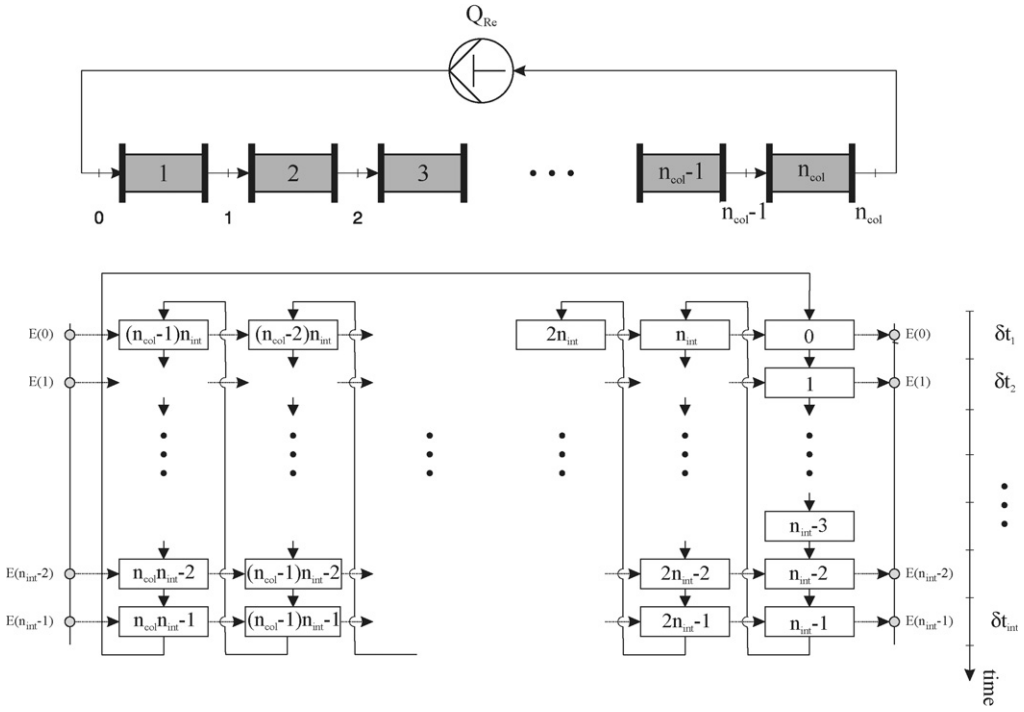

Fig. 9. Formulation of the stages in Method II.

5.3.2. Approximation

The temporal evolution of the inlet concentration $c_{\text{in},n_s}(t)$ of species n_s is approximated using Legendre polynomials according to (see Appendix B):

$$c_{\text{in},n_s}(t) = \sum_{l=1}^{n_{\text{Le}}} q^l_{\text{in},n_s} \phi_l(t) = \mathbf{q}^{\text{T}}_{\text{in},n_s} \Phi(t), \quad n_s = 1, \ldots, n_{\text{sp}} \tag{37}$$

with the Legendre coefficients $\mathbf{q}_{\text{in},n_s}$ and the Legendre basis functions $\Phi(t)$:

$$\mathbf{q}_{\text{in},n_s} = [q^1_{\text{in},n_s}, q^2_{\text{in},n_s}, \ldots, q^{n_{\text{Le}}}_{\text{in},n_s}], \quad n_s = 1, \ldots, n_{\text{sp}} \tag{38}$$

$$\Phi(t) = [\phi_1(t), \phi_2(t), \ldots, \phi_{n_{\text{Le}}}(t)]^{\text{T}} \tag{39}$$

n_{Le} denotes the number of Legendre polynomials considered. Eq. (37) yields additional algebraic equations in the DAE system (34).

In order to connect the chromatographic columns and to impose the node restrictions, the outlet concentration must also be approximated by Legendre polynomials of the same order. That is the reason why the Legendre coefficients $\mathbf{q}_{\text{out},n_s}$ are introduced as additional states. Due to the orthogonality of the Legendre polynomials (see Appendix B), the following relationship holds:

$$\mathbf{q}_{\text{out},i} = \int_0^1 c_{\text{out},i}(t)\Phi(t), \quad i = 1, \ldots, n_{\text{sp}}\, \text{d}t \tag{40}$$

Differentiation with respect to time yields the additional differential equations in the DAE-system (34).

Finally, $\Delta\mathbf{c}_{\text{out}}$ denotes the approximation error. It is evaluated according to

$$\Delta c_{\text{out},i}(t) = c_{\text{out},i}(t) - \mathbf{q}^{\text{T}}_{\text{out},i}\Phi(t), \quad i = 1, \ldots, n_{\text{sp}} \tag{41}$$

In Fig. 11 the concentration profiles collected at a fixed position in the SMB loop are compared to their respective Legendre approximations. In this case, a two-stage SMB process with three Legendre coefficients per stage was considered. The error between the exact and the approximated profiles is negligible and the Legendre approximation is fitting well also the steep fronts, e.g. in columns 3 and 7.

5.3.3. Constraints

The relationships listed in Table 2 are used here for the evaluation of the objective function and the purity constraints.

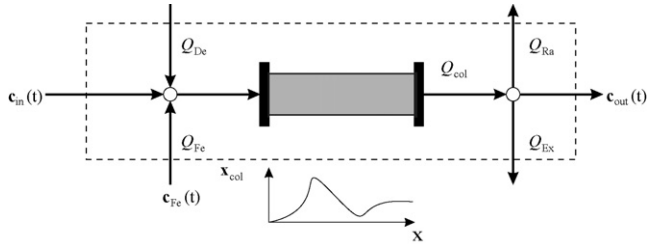

Fig. 10. Input/output variables of a chromatographic column.

Table 2
Optimization settings

Configuration	2/2/2/2
Target	max(Pr)
	$\text{Pur}_{\text{Ex, min}} = 99.5\%$
	$\text{Pur}_{\text{Ra, min}} = 99.5\%$
Constraints	$Q_{\text{max}} = 500$ ml/min
	$Q_{\text{min}} = 20$ ml/min
	$n_{\text{col}} = 8$
	$\tau_{\text{min}} = 0.5$ min

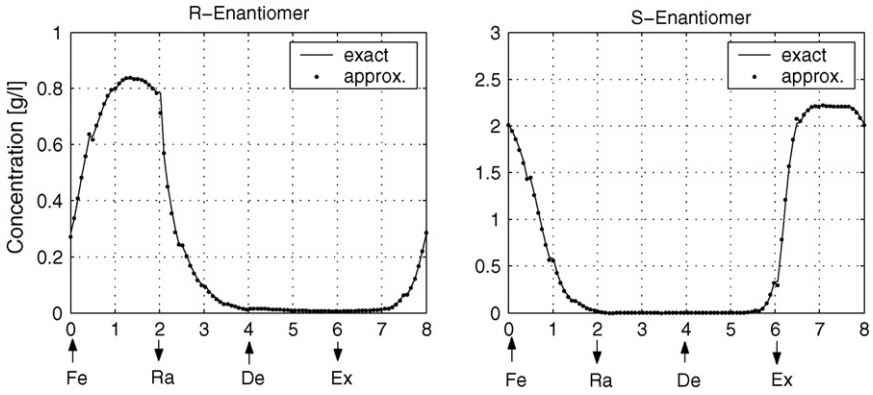

Fig. 11. Legendre approximation.

Additionally, the flow rates in the chromatographic columns must be strictly positive (as it appears in the denominator of the GRM-model), and it has an upper-bound due to the pressure drop. Thus for stage k ($k = 0, \ldots, n_{\mathrm{col}} n_{\mathrm{int}} - 1$):

$$Q_{\min} \leq Q_{\mathrm{col}} = Q_{\mathrm{int}} + Q_{\mathrm{De}} + Q_{\mathrm{Fe}} \leq Q_{\max} \tag{42}$$

The cyclic steady state constraint is for the most part represented by continuity conditions between the stages. What remains is to couple the last stage to the first one. These additional equalities are formulated as multipoint constraints between stage 0 and stage $n_{\mathrm{col}} n_{\mathrm{int}} - 1$:

$$\mathbf{x}_{\mathrm{col}}^{0}(t = 0) = \mathbf{x}_{\mathrm{col}}^{n_{\mathrm{col}} n_{\mathrm{int}} - 1}(t = \tau) \tag{43}$$

In addition, according to Fig. 9, the outlet concentrations of stage $(k + n_{\mathrm{int}})$ are the inlet concentrations of stage k. The same holds for the flow rates between stage k and stage k'. For $k = 0, \ldots, n_{\mathrm{col}} n_{\mathrm{int}} - 1$:

$$k' = \mathrm{mod}\,(k + n_{\mathrm{int}}, n_{\mathrm{col}} n_{\mathrm{int}} - 1) \tag{44}$$

$$q_{\mathrm{in},n_s}^{k} = q_{\mathrm{out},n_s}^{k'}(\tau) - q_{\mathrm{out},n_s}^{k'}(0) \tag{45}$$

$$Q_{\mathrm{int}}^{k} = Q_{\mathrm{int}}^{k'} - Q_{\mathrm{Ra}}^{k'} - Q_{\mathrm{Ex}}^{k'} + Q_{\mathrm{Fe}}^{k'} + Q_{\mathrm{De}}^{k'} \tag{46}$$

$$\Delta c_{\mathrm{out},n_s}^{k} = c_{\mathrm{out},n_s}^{k} - (\mathbf{q}_{\mathrm{out},ns}^{k}(\tau) - \mathbf{q}_{\mathrm{out},ns}^{k}(0))^{\mathrm{T}} \Phi(t) \tag{47}$$

where $\mathrm{mod}(l, m)$ denotes the modulus function, often also written l (mod m).

Since the normalized Legendre polynomials are defined in the interval [0,1], the durations of the stages are normalized. Additional parameters δt_i are added to the dynamic equations of the chromatographic column to scale the model equations to the interval [0,1]. The stages of each sub-interval i are synchronized by the following additional equality constraints for $i = 0, \ldots, n_{\mathrm{int}}$:

$$\delta t_{i+jn_{\mathrm{int}}} = \delta t_i, \quad j = 1, \ldots, n_{\mathrm{col}} - 1 \tag{48}$$

6. Numerical study

We consider the non-linear enantiomer mixture EMD-53986 as a case study to compare the different optimization approaches. EMD-53986 exhibits a non-linear adsorption isotherm that can be approximated well by an extended Langmuir isotherm [3,61]:

$$q_i = H_i^1 c_{\mathrm{p},i} + \frac{H_i^2 c_{\mathrm{p},i}}{n_{\mathrm{sp}}} \Big/ \left(1 + \sum_{j=1} k_j^2 c_{\mathrm{p},j}\right) \tag{49}$$

The parameters were taken from the thesis of Jupke [61] and are summarized in Appendix D. The design settings are listed in Table 2. The productivity is considered here as the performance criterion. The purities at both product lines must be kept higher than 99.5%. Lower and upper bounds are prescribed for the internal column flow rates. The switching time τ is constrained to be at least 30 s in order to avoid too frequent valve switching, and the SMB process is composed of eight chromatographic columns.

Appendix D lists the system parameters and the operating point used to initialize the optimization runs. The integrator tolerances were set to 10^{-5}. In the sequential approach, the upper mass balance error is set to 0.25% and the tolerance for the cyclic steady state corresponds to 3.0×10^{-4}. Ten finite elements for the fluid phase and one internal collocation point for the particle phase were chosen for spatial discretization so that an ODE-system with 672 state variables results for the SMB process. Numerical studies showed that one internal collocation point is sufficient to approximate the concentration profile in the particle phase which is dominated by fast particle diffusion.

Table 3 compares the numerical performance of the different approaches when applied to the classical one-stage SMB process. MUSCOD-II and FFSQP can only solve minimiza-

Table 3
Numerical performance of the different approaches (one-stage SMB process)

	Sequential	Method I	Method II
Normalized objective	1.925	1.950	**1.935**
Computation time [min]	18.87	21.93	**9.42**
Number of iterations	12	11	**16**
Comp. time per iteration [s]	94	120	**35**
No. of optimization variables	5	1362	**964**
No. of equality constraints	–	1357	**959**
No. of inequality constraints	13	2742	**1946**

Table 4
Comparison of the simultaneous approaches for multi-stage SMB processes

n_{int}	Normalized objective function		Computation time (s)		Number of SQP iterations		Computation time per iteration (s)	
	Method I	Method II	Method I	Method II	Method I	Method II	Method I	Method II
1	1.950	1.935	1,316	565	11	16	120	35
2	2.180	2.161	9,178	3,857	43	73	213	53
3	2.192	2.174	13,289	4,273	41	70	324	61
4	2.222	2.204	9,616	5,349	27	63	356	85
5	2.221	2.217	22,117	8,590	53	77	417	112
6	2.226	2.216	28,946	11,565	56	85	517	136
7	2.223	2.221	18,453	6,831	34	36	543	190
8	2.221	2.219	24,325	24,116	39	94	624	257
9	2.223	2.223	57,697	14,768	82	54	704	273
10	2.222	2.225	79,139	25,747	101	75	784	343

tion problems. Maximizing the productivity is therefore simply transformed to minimizing the negative productivity. The normalized objective function listed in the first row of Table 3 is the ratio between the optimal productivity and a reference productivity. The reference productivity is to the productivity of the initial operating point from which all optimization runs were started (see Appendix D). Table 3 indicates how small the sequential optimization problem is in comparison to both simultaneous approaches since the periodicity conditions are hidden from the optimization stage. However, the calculation time required by the sequential approach and Method I are approximately identical despite the large size of the optimization problem arising in Method I. It has to be noted that all three approaches converge to an approximately identical operating point. In Method II, three Legendre polynomials were considered. In comparison to Method I, Method II reduces the dimension of the differential equation system drastically while maintaining the accuracy of the solution. This lead to a decrease of the overall calculation time by more than factor 2. The CPU-time required for one iteration is reduced by a higher factor of 2.6.

The extension of the sequential approach to a multi-stage SMB process with modulation of the flow rates (PowerFeed) leads to a larger optimization problems. As discussed before, a finite difference scheme is used in this case for gradient computation which lead to an increase of the calculation time which is at least linear in the number of optimization variables. Table 4 compares the numerical performance of the different strategies for a multi-stage SMB process. In Fig. 12, additionally to the numerical results for the simultaneous approaches, the extrapolated calculation times for the sequential approach are also shown.

It should be pointed out that the higher the number of stages n_{int}, the closer is the approximated solution to the exact one. This is due to the fact that the whole period length (sum of all intervals) does not change a lot when the number of stages increases, whereas with each new interval further Legendre polynomials are added leading to a better approximation of the inlet/outlet concentrations. Method II in all cases needs absolutely less computing time than Method I. This is mainly a consequence of the smaller size of the differential equation system which leads to a reduction in the computation time per iteration by a factor of 2.3–5.3, as can be seen by comparing the last two columns of Table 4, see also Fig. 12.

The absolute number of SQP iterations until the termination criterion is met (see Table 4) is difficult to predict and varies considerably. However, it can be seen that it only slightly increases with the number of stages n_{int}, and that it is in the same order of magnitude for Methods I and II, indicating no deterioration of the convergence properties due to Method II. Summarizing, Method II is faster because it has a smaller cost per iteration and at the same time does not increase the total number of iterations. In Fig. 12, it can be seen that its cost per iteration are always smaller than for the sequential approach.

The gain in numerical performance and efficiency by Method II enabled us to optimize the more challenging operating regimes VARICOL and PowerFeed. Fig. 13 shows the optimal operating point obtained for a 10-stage SMB Process which is equivalent to the PowerFeed process with 10 time-intervals. In this study, the maximal flow rate Q_{max} was set to 18,ml/min and equidistant time-intervals were imposed. As can be seen from Fig. 13 and was confirmed by several

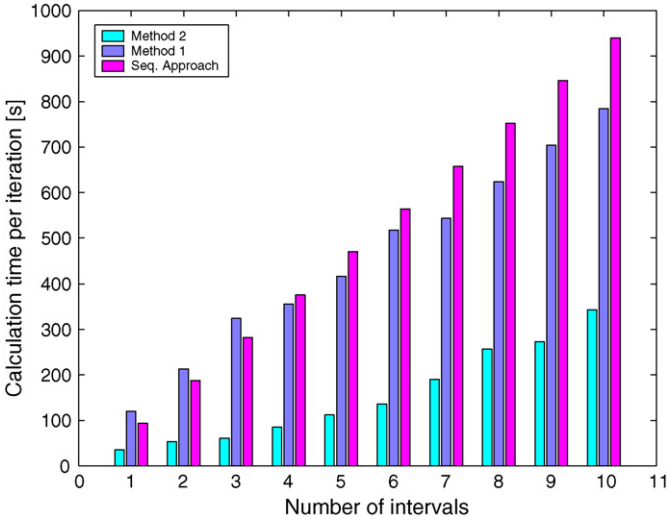

Fig. 12. Calculation time per iteration for the different optimization strategies.

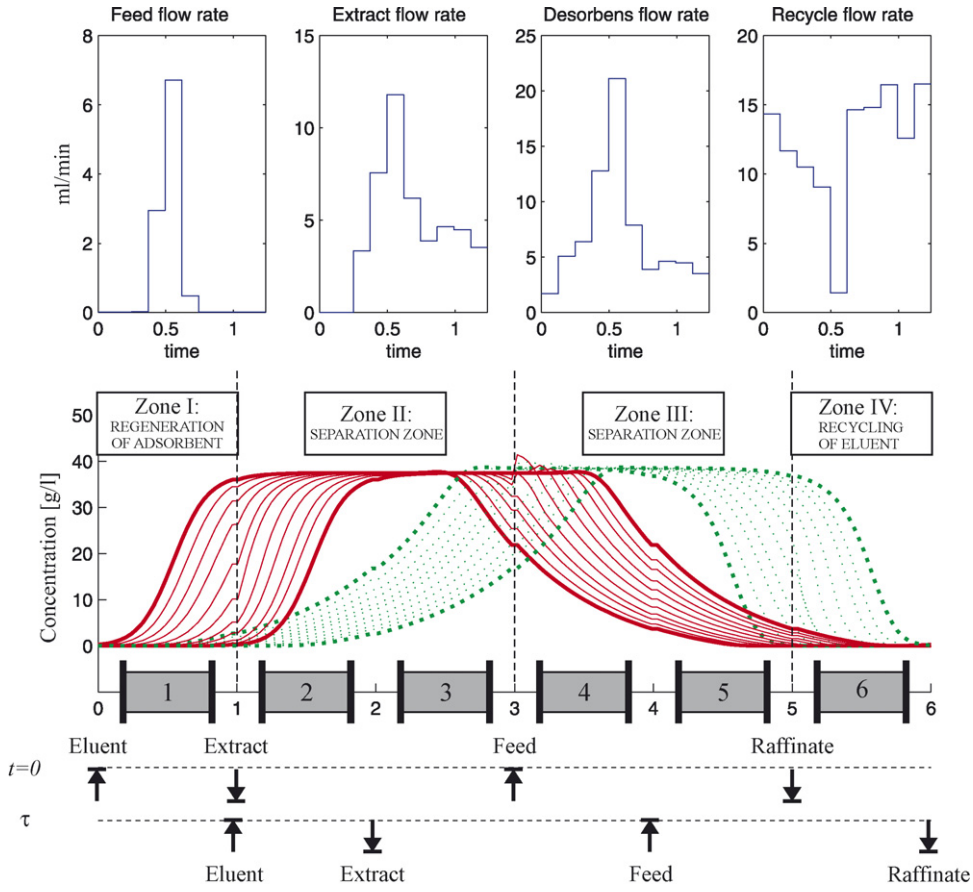

Fig. 13. Optimal operating regime for a 10-stage SMB process (PowerFeed).

other optimization runs, the optimal operating point is mainly characterized by the following features:

- The feed flow rate reaches its maximum in the middle of the switching period and it is approximately zero at the beginning and at the end of the period.
- At the beginning of the period, the extract port is closed and pure raffinate is withdrawn.
- Toward the end of the switching period, the raffinate port is closed and pure extract is withdrawn.

A batch-wise injection and withdrawal leads to a better performance than a continuous operation where all inlet/outlet lines at each time instant are transporting material. The optimal chromatographic multi-stage SMB process is a combination of batch and continuous operation. The plotted axial concentration profiles explain this point more clearly. When a high productivity is envisaged, the columns are overloaded and the distance between the concentration fronts is lower than one column length. At the beginning of the switching period, the less-retained component is therefore present in zone I, so extract withdrawal has to be delayed until this front leaves the first zone. In the mean time, raffinate can be withdrawn since the more retained component is still far away from the raffinate port. Once the polluting front reaches the raffinate outlet, the raffinate port has to be closed. In summary, the PowerFeed process is able to better adapt the flow rates to overloaded concentration profiles, thus maintaining the purity requirements while enhancing the productivity.

As indicated in Table 5, the four-stage PowerFeed process reaches a productivity enhancement of 13.8% in comparison to the classical SMB process. The column configuration 2/2/2/2 was used in both cases. An asynchronous switching of the inlet/outlet lines realized by the VARICOL process increases the productivity additionally by 10.4%. The combination of PowerFeed and VARICOL is thus a promising alternative to the classical SMB process leading to altogether 24.2% higher productivity while providing high operational flexibility.

Table 5
Comparison of PowerFeed and VARICOL

Process	SMB	PowerFeed	VARICOL
n_{int}	1	4	4
Normalized objective function	1.935	2.204	2.405
Relative productivity gain (%)	–	13.8	24.2
Computation time (min)	9.42	88.78	84.66
Number of iterations	16	71	66
Computation time per iteration (s)	35	75	77
No. of optimization variables	964	3535	3535
No. of equality constraints	959	3515	3515
No. of inequality constraints	1946	7136	7136

7. Summary and future work

Chromatography has developed from an analytical to a well-established preparative separation technique in industry. It is the method of choice for difficult separation tasks especially when temperature-sensitive components or species exhibiting similar thermodynamic properties are involved. Large-scale industrial applications have been reported from different industrial fields, e.g. in the petro-chemical, pharmaceutical, bio-chemical, and also in the food industry. SMB processes have gained more and more attention due to their advantages in terms of solvent consumption and productivity.

SMB processes often cause a large fraction of the overall production cost, so their efficient design and operation become mandatory when production cost matters for competitiveness. In this paper, we developed an efficient and reliable optimization strategy based on the multiple shooting method. It incorporates realistic, detailed process models and rigorous solution procedures. The multiple shooting method enables the simultaneous computation of the state trajectory and of the operating parameters avoiding the time-consuming convergence to the cyclic steady state in each iteration. Thanks to a new problem formulation where a large part of the CSS is imposed directly and the inlet/outlet concentrations are approximated by Legendre polynomials, the computation times could be drastically reduced by a factor of 2–4. A classical SMB process with more than 600 differential states was optimized in less than 10 min CPU-time.

The availability of an efficient numerical method enabled us to explore the potential of more challenging operating regimes as, e.g. VARICOL and PowerFeed. An enantiomer separation with a non-linear extended Langmuir isotherm was considered as a case study. The optimal multi-stage SMB process consists of a combination of batch and continuous operation. It was found out that a batch-wise injection of feed and withdrawal of extract and raffinate during a switching period is advantageous in terms of productivity. A combination of VARICOL and PowerFeed leads to more than 20% higher productivity. We believe that by applying the new efficient numerical strategies developed in this article, the high flexibility offered by VARICOL and PowerFeed can be further exploited in practice and research, saving costs and time.

The multiple shooting method can also be adapted for online optimization [28]. In the context of online optimization three further issues are of great importance: state estimation, online solution of the optimization problems and stability guarantees. These topics are subject of the research cluster "Optimization-based control of chemical processes" which is sponsored by the German Research Council and includes groups from Aachen (Marquardt), Heidelberg (Bock/Diehl/Schlöder), Stuttgart (Allgöwer) and Dortmund (Engell).

Acknowledgements

The financial support of Deutsche Forschungsgemeinschaft in the context of the research cluster "Optimization-based control of chemical processes" under grants En 152/34 and Bo 864/10 is very gratefully acknowledged.

Appendix A. Nomenclature

$\mathbf{c}_\mathrm{b}$	concentration in the bulk (fluid) phase
$\mathbf{c}_\mathrm{p}$	concentration in the particle phase
$\mathbf{c}^\mathrm{in}$	concentration at the inlet of the column
$\mathbf{c}^\mathrm{out}$	concentration at the outlet of the column
$\mathbf{c}_i^\mathrm{eq}$	equilibrium concentrations
Δc_out	quality of Legendre-approximation
$\mathrm{Cost}_\mathrm{spec}$	specific costs
D_ax	axial dispersion
D_p	particle diffusion coefficient
$\mathbf{f}$	continuous dynamic
$\mathbf{h}$	measurement function
H_i	Henry coefficient of component i
k_j	Langmuir constants (denominator terms)
k_l	film mass transfer resistance coefficient
L	column length
m	integral masses leaving or entering a column
m_css	mass balance mismatch in percent
M	number of sub-intervals
n_c	number of collocation points
n_col	number of columns
n_fe	number of finite elements
n_int	number of intervals
n_sp	number of species
$\mathrm{neq}_\mathrm{col}$	number of ODE-equations (single column)
$\mathrm{neq}_\mathrm{smb}$	number of ODE-equations (SMB)
$\mathbf{p}$	parameter vector
Pr	productivity
Pur	purity
q_i	adsorbed quantity per amount of adsorbent
q_in	Legendre coefficients
q_out	Legendre coefficients
Q	flow rate
Q_max	maximal flow rate in a chromatographic column
r	radial coordinate
R_p	particle radius
t	time
u	interstitial velocity
$\mathbf{u}$	control vector
x	axial coordinate
$\mathbf{x}$	state vector

Greek letters

δt	interval length
ε_b	bulk porosity
ε_p	particle porosity
ε_css	cyclic steady state tolerance
ϕ	Legendre polynomial
Φ	Legendre basis
Γ	dynamic operator (CSS)
τ	switching period

Subscripts

col	column
De	desorbent
Ex	extract

Fe	feed
int	interval or intermediate
max	maximal
min	minimal
Ra	raffinate
spec	specific
smb	simulated moving bed

Appendix B. Legendre polynomials

The Legendre polynomials ϕ_l are defined recursively according to

$$\phi_l(t) = \sqrt{2l-1}\phi_l^*(t), \quad l = 1, \ldots, n_{\mathrm{Le}} \tag{50}$$

with

$$\phi_1^*(t) = \phi_2^*(t) = (2t-1), \quad \text{and for } l = 3, \ldots, n_{\mathrm{Le}},$$
$$\phi_l^*(t) = \frac{2l-3}{l} t\phi_{l-2}^*(t) - \frac{(l-2)}{l}\phi_{l-3}^*(t) \tag{51}$$

Being an orthonormal basis, the Legendre polynomials exhibit the following relationships:

$$\int_0^1 \phi_l(t)\phi_k(t)\,\mathrm{d}t = 0, \qquad \int_0^1 \phi_l^2(t)\,\mathrm{d}t = 1,$$
$$(k,l) = 1, \ldots, n_{\mathrm{Le}}, \quad k \neq l \tag{52}$$

Appendix C. Permutation matrix

The permutation matrix **P** is given by

$$\mathbf{P} = \begin{pmatrix} \mathbf{0} & \cdots & \cdots & \mathbf{0} & \mathbf{I} \\ \mathbf{I} & \ddots & \mathbf{0} & \cdots & \mathbf{0} \\ \mathbf{0} & \mathbf{I} & \ddots & \ddots & \vdots \\ \vdots & \ddots & \mathbf{I} & \ddots & \mathbf{0} \\ \mathbf{0} & \cdots & \mathbf{0} & \mathbf{I} & \mathbf{0} \end{pmatrix}$$

I denotes the $(\mathrm{neq_{col}}, \mathrm{neq_{col}})$-identity matrix and n is the number of state variables of a single chromatographic column. n_{col} denotes the total number of chromatographic columns.

Appendix D. EMD-53986

EMD-53986 is a chemical abbreviation for the enantiomer (5-(1,2,3,4-tetrahydroquinoline-6-yl)-6-methyl-3,6-dihydro-1,3,4-thiadiazine-2-one).

The isotherm was experimentally validated in cooperation with *M* erck (Germany) and the Chair of Process Design (Universität Dortmund). It was considered as a case study in the research cooperation "Optimal operation and model-based control of chromatographic processes" which was financially supported by the Bundesministerium für Bildung und Forschung (BMBF) [62]. The parameters were taken from the thesis of Jupke [61] and are shown in Table D.1.

Table D.1
Parameters for the enantiomer mixture EMD-53986

System parameters	
Column length, L (cm)	9.0
Particle porosity, ε_{p}	0.567
Particle diameter, R_{p} (μm)	1.0
Mass transfer coefficient, $k_{l,\mathrm{A}}$ (s^{-1})	1.5E−4
Extended Langmuir isotherm	$H_i^1 c_i + \frac{H_i^2 c_i}{1+\sum k_k^2 c_k}$
Henry coefficient, H_{B}^1	2.054
Henry coefficient, H_{B}^2	5.847
Isotherm parameter, k_{B}^2 (cm^3/g)	129.0
Viscosity methanol, ν (g/(cm s))	1.2E−2
Column diameter, D (cm)	2.5
Bed porosity, ε_{b}	0.353
Diffusion coefficient, D_{p} (cm^2/s)	1.0E−3
Mass transfer coefficient, $k_{l,\mathrm{B}}$ (s^{-1})	2.0E−4
Henry coefficient, H_{A}^1	2.054
Henry coefficient, H_{A}^2	19.902
Isotherm parameter, k_{A}^2 (cm^3/g)	472.0
Density methanol, ρ (g/cm^3)	0.799
Particle diffusion, D_{p} (cm^2/s)	1.0E−3
Operating parameters	
Flow rate, $Q_{\mathrm{max},1}$ (ml/min)	500.0
Column configuration, N_i	[2 2 2 2]
Des. flow rate, Q_{De} (ml/min)	123.6
Raffinate flow rate, Q_{Ra} (ml/min)	24.1
Period, τ (min)	2.433
Extract purity, $\mathrm{Pur_{Ex}}$ (%)	99.936
Feed flow rate, Q_{Fe} (ml/min)	14.5
Feed concentration, $c_{\mathrm{Fe},i}$ (g/l)	[2.5, 2.5]
Rec. flow rate, Q_{Re} (ml/min)	42.0
Extract flow rate, Q_{Ex} (ml/min)	114.0
β-Factors, β_i	0.6,0.5,4.1,2.6
Raffinate purity, $\mathrm{Pur_{Ra}}$ (%)	99.606
Numerical parameters	
Collocation points, n_{c}	1
Rel. integr. tol., r_{tol}	1.0E−5
Steady state tol., $\varepsilon_{\mathrm{css}}$	3.0E−4
Finite elements, n_{fe}	10
Abs. integr. tol., a_{tol}	3.0E−5
Max. mass bal., m_{css}	0.25

A: *R*-Enantiomer; B: *S*-Enantiomer.

The axial dispersion coefficient $D_{\mathrm{ax},i}$ is calculated according to the empirical correlation of the Peclet- and the particle Reynolds number [63]:

$$D_{\mathrm{ax}} = \frac{2u R_{\mathrm{p}}}{Pe} \tag{53}$$

with

$$Pe = \frac{0.2}{\varepsilon_{\mathrm{b}}} + \frac{0.011}{\varepsilon_{\mathrm{b}}}[Re_{\mathrm{p}}\,\varepsilon_{\mathrm{b}}]^{0.48}, \quad Re_{\mathrm{p}} = \frac{2u R_{\mathrm{p}}\rho}{\nu} \tag{54}$$

References

[3] J. Strube, A. Jupke, A. Epping, H. Schmidt-Traub, M. Schulte, R. Devant, Design, optimization and operation of chromatographic processes in the production of enantiomerically pure pharmaceuticals, Chirality 11 (1999) 440–450.

[4] S. Imamoglu, Simulated moving bed chromatography (SMB) for applications in bioseparation, Adv. Biochem. Eng. Biotechnol. 76 (2002) 211–231.

[6] D. Leineweber, Efficient reduced SQP methods for the optimization of chemical processes described by large sparse DAE models, Dissertation, vol. 613, VDI Reihe 3, Verfahrenstechnik, VDI Verlag, 1999.
[7] H. Bock, K. Plitt, A multiple shooting algorithm for direct solution of optimal control problems, in: Proceedings of the 9th IFAC World Congress Budapest, Pergamon Press, 1984, pp. 243–247.
[10] Z. Zhang, M. Mazzotti, M. Morbidelli, PowerFeed operation of simulated moving bed units: changing flow-rates during the switching interval, J. Chromatogr. A 1006 (2003) 87–99.
[11] Y. Xie, Y. Koo, N. Wang, Preparative chromatographic separation: simulated moving bed and modified chromatography methods, Biotechnol. Bioprocess Eng. 6 (2001) 363–375.
[12] M. Juza, Development of a high-performance liquid chromatographic simulated moving bed separation from an industrial perspective, J. Chromatogr. A 865 (1999) 35–49.
[13] M. Juza, M. Mazzotti, M. Morbidelli, Simulated moving-bed chromatography and its application to chirotechnology, Trends Biotechnol. 18 (2000) 108–118.
[14] D. Pavone, G. Hotier, System approach modelling applied to the eluxyl process, Oil Gas Sci. Technol. 55 (2000) 437–446.
[15] R. Wooley, Z. Ma, N. Wang, A nine-zone simulating moving bed for the recovery of glucose and xylose from biomass hydrolyzate, Ind. Eng. Chem. Res. 37 (1998) 3699–3709.
[16] S. Baudouin, X. Lancrenon, Désucrage des égouts et des mélasses, Ind. Aliment. Agric. 120 (2003) 42–48.
[17] E.R. Francotte, P. Richert, Applications of simulated moving-bed chromatography to the separation of the enantiomers of chiral drugs, J. Chromatogr. A 769 (1997) 101–107.
[18] M. McCoy, SMB emerges as chiral technique, Chem. Eng. News 78 (2000) 17–19.
[19] C. Migliorini, M. Mazzotti, M. Morbidelli, Continuous chromatograpic separation through simulated moving beds under linear and nonlinear conditions, J. Chromatogr. A 827 (1998) 161–173.
[20] C. Migliorini, M. Mazzotti, M. Morbidelli, Design of simulated moving bed multicomponent separations: Langmuir systems, Sep. Purif. Technol. 20 (2000) 79–96.
[21] L. Miller, C. Grill, T. Yan, O. Dapremont, E. Huthmann, M. Juza, Batch and simulated moving bed chromatographic resolution of a pharmaceutical racemate, J. Chromatogr. A 1006 (2003) 267–280.
[22] G. Dünnebier, J. Fricke, K.-U. Klatt, Optimal design and operation of simulated moving bed chromatographic reactors, Ind. Eng. Chem. Res. 39 (2000) 2290–2304.
[23] G. Dünnebier, K.-U. Klatt, Modelling and simulation of nonlinear chromatographic separation processes: A comparison of different modelling approaches, Chem. Eng. Sci. 55 (2000) 373–380.
[24] G. Guiochon, Preparative liquid chromatography, J. Chromatogr. A 965 (2002) 129–161.
[25] T. Gu, Mathematical Modelling and Scale Up of Liquid Chromatography, Springer, New York, 1995.
[26] G. Erdem, S. Abel, M. Morari, M. Mazzotti, M. Morbidelli, Automatic control of simulated moving beds. II. Nonlinear isotherm, Ind. Eng. Chem. Res. 43 (14) (2004) 3895–3907.
[27] S. Abel, G. Erdem, M. Mazzotti, M. Morari, M. Morbidelli, Optimizing control of simulated moving beds—linear isotherm, J. Chromatogr. A 1033 (2) (2004) 229–239.
[28] A. Toumi, M. Diehl, S. Engell, H. Bock, J. Schlöder, Finite Horizon Optimizing Control of Advanced SMB Chromatographic Processes, in: Proceedings of the IFAC World Congress, Prague, 2005 (CD ROM).
[29] A. Toumi, S. Engell, O. Ludemann-Hombourger, R.M. Nicoud, M. Bailly, Optimization of simulated moving bed and VARICOL processes, J. Chromatogr. A 1006 (2003) 15–31.
[30] L. Biegler, Efficient solution of dynamic optimization and NMPC problems, in: F. Allgöwer, A. Zheng (Eds.), Nonlinear Model Predictive Control, Birkhäuser Verlag, Basel, 2000, pp. 219–243.
[31] D. Leineweber, A. Schäfer, H. Bock, J. Schlöder, An efficient multiple shooting based reduced SQP strategy for large-scale dynamic process optimization. Part II. Software aspects and applications, Comp. Chem. Eng. 27 (2003) 167–174.
[32] D.W. Guest, Evaluation of simulated moving bed chromatography for pharmaceutical process development, J. Chromatogr. A 760 (1997) 159–162.
[33] D. Broughton, C.G. Gerhold, Continuous sorption process employing fix beds of sorbent and moving inlets and outlets, US Patent 2,985,589 (1961).
[34] R. Nicoud, R. Majors, Simulated moving bed chromatography for preparative separations, LCGC 18 (7) (2000) 680.
[35] F. Lode, M. Houmard, C. Migliorini, M. Mazzotti, M. Morbidelli, Continuous reactive chromatography, Chem. Eng. Sci. 56 (2001) 269–291.
[36] G. Biressi, F. Quattrini, M. Juza, M. Mazzotti, V. Schurig, M. Morbidelli, Gas chromatographic simulated moving bed separation of the enantiomers of the inhalation anesthetic enflurane, Chem. Eng. Sci. 55 (2000) 4537–4547.
[37] F. Denet, W. Hauck, R.M. Nicoud, O.D. Giovanni, M.M.J.N. Jaubert, M. Morbidelli, Enantioseparation through supercritical simulated moving bed (SF-SMB) chromatography, Ind. Eng. Chem. Res. 40 (2001) 4603–4609.
[38] M. Villeneuve, P. Williams, Chiral and achiral separations using the new novasep supercritical fluid chromatography, in: Proceedings of the 16th International Symposium on Preparative Chromatography, San Francisco, USA, June 29 to July 02, 2003.
[39] O. Ludemann-Hombourger, R.M. Nicoud, The VARICOL process: a new multicolumn continuous chromatographic process, Sep. Sci. Technol. 35 (2000) 1829–1862.
[40] O. Ludemann-Hombourger, G. Pigorini, R. Nicoud, D. Ross, G. Terfloth, Application of the VARICOL process to the separation of the isomers of the SB-553261 racemate, J. Chromatogr. A 947 (2002) 59–68.
[41] H. Schramm, M. Kaspereit, A. Kienle, A. Seidel-Morgenstern, Improving simulated moving bed processes by cyclic modulation of the feed concentrations, Chem. Eng. Technol. 25 (2002) 1151–1155.
[42] G. Ganetsos, P.E. Barker, J.N. Ajongwen, Batch and continuous chromatographic systems as combined bioreactor-separators, in: G. Ganetsos, P.E. Barker (Eds.), Preparative and Production Scale Chromatography, Marcel Dekker, New York, 1993, pp. 375–393.
[43] A.C. Hindmarsh, ODEPACK, a systematized collection of ODE solvers, in: R.S. Stepleman (Ed.), Scientific Computing, North-Holland, Amsterdam, 1983, pp. 55–64.
[44] A. Toumi, F. Hanisch, S. Engell, Optimal operation of continuous chromatographic processes: mathematical optimization of the VARICOL process, Ind. Eng. Chem. Res. 41 (2002) 4328–4337.
[45] S. Nilchan, C. Pantelides, On the optimisation of periodic adsorption processes, Adsorption 4 (1998) 113–147.
[46] H. Bock, M. Diehl, D. Leineweber, J. Schlöder, A direct multiple shooting method for real-time optimization of DAE processes, in: F. Allgöwer, A. Zheng (Eds.), Nonlinear Model Predictive Control, Birkhäuser Verlag, Basel, 2000, pp. 246–267.
[47] L. Jiang, L. Biegler, V. Fox, Simulation and optimization of pressure-swing adsorption systems for air separation, AIChE J. 49 (2003) 1140–1157.
[48] E. Kloppenburg, Modellbasierte Prozessführung von Chromatographieprozessen mit simuliertem Gegenstrom, Dissertation, Fortschritt Berichte VDI-Verfahrenstechnik, Universität Stuttgart, 2000.
[49] K. Mohl, A. Spieker, E. Stein, E. Gilles, DIVA-eine Umgebung zur Simulation, Analyse und Optimierung verfahrenstechnischer Prozesse, in: A. Kuhn, S. Wenzel (Eds.), Proceedings of the Simulationstechnik, 11. ASIM-Symposium in Dortmund, Vieweg Verlag, Braunschweig/Wiesbaden, 1997, pp. 278–283.
[50] P. Deuflhard, U. Nowak, M. Wulkow, Recent developements in chemical computing, Comput. Chem. Eng. 14 (1990) 1249–1258.
[51] R. Fourer, D. Gay, B. Kernighan, AMPL, A Modeling Language for Mathematical Programming, Boyd and Fraser Publishing Company, 1993.
[52] A. Conn, Lancelot—A FORTRAN Package for Large-Scale Nonlinear Optimization (Release A), Springer-Verlag, Berlin, 1992.
[53] E. Kloppenburg, E.D. Gilles, Ein neues Prozessführungskonzept für die Chromatographie mit simuliertem Gegenstrom, Chem. Ing. Tech. 70 (1998) 1526–1529.
[54] M. Minceva, L. Pais, A. Rodrigues, Cyclic steady state of simulated moving bed processes for enantiomers separation, Chem. Eng. Process. 42 (2003) 93–104.
[55] R. Leveque, Numerical Methods for Conservation Laws, Birkhäuser Verlag, Basel, 1992.

[56] M. Diehl, D.B. Leineweber, A.S. Schäfer, MUSCOD-II User's Manual, Preprint 2001–25, Interdisziplinäres Zentrum für wissenschaftliches Rechnen, Heidelberg, 2001.
[57] I. Bauer, H.G. Bock, D.B. Leineweber, J.P. Schlöder, Direct multiple shooting methods for control and optimization of DAE in chemical engineering, Sci. Comput. Chem. Eng. II: Simul. Image Process. Optimizat. Contr. (1999) 2–18.
[58] A. Toumi, S. Engell, (2003). SMBOpt: a software package for optimal operation of chromatographic simulated moving bed processes, in: H.G. Bock, E. Kostina, H.X. Phu, R. Rannacher (Eds.), Modelling, Simulation and Optimization of Complex Processes, Proceedings of the International Conference on High Performance Scientific Computing, March 10–14, 2003, Hanoi, Vietnam, Springer, 2004.
[59] J.L. Zhou, A.L. Tits, C.T. Lawrence, User's Guide for FFSQP Version 3.7: A FORTRAN Code for Solving Constrained Nonlinear (Minimax) Optimization Problems, Generating Iterates Satisfying all Inequality and Linear Constraints, University of Maryland, 1997.
[60] R. Todd, J. He, P. Webley, C. Beh, S. Wilson, M. Lloyd, Fast finite-volume method for PSA/VSA cycle simulation—experimental validation, Ind. Eng. Chem. Res. 40 (2001) 3217–3224.
[61] A. Jupke, Experimentelle Modellvalidierung und Modellbasierte Auslegung von Simulated Moving Bed (SMB) Chromatographieverfahren, Dissertation, Universität Dortmund, Fachbereich Bio- und Chemieingenieurwesen, 2002.
[62] S. Engell, H. Schmidt-Traub, R. Ditz, Optimale Prozeßführung und modellbasierte Regelung von Chromatographie-Prozessen unter Einsatz von Methoden der nichtlinearen Systemtheorie, Abschlussbericht, BMBF-Projekt 03D0062B0/03D0062A7, 2001.
[63] S. Chung, C. Wen, Longitudinal diffusion of liquid flowing through fixed and fluidized beds, AIChe J. 14 (1968) 857–866.

Further reading

[1] SDI, Preparative and Process Liquid Chromatography: The Future of Process Separations, International Strategic Directions, Los Angeles, USA, 2002. http://www.strategic-directions.com.
[2] J. Kinkel, M. Schulte, R. Nicoud, F. Charton, Simulated moving bed (SMB) chromatography: an efficient method for performing large-scale separation of optical isomers, Chiral Eur. 95 (1995) 121–132.
[5] A. Toumi, Optimaler Betrieb und Regelung von Simulated Moving Bed Prozessen, Dissertation, Fachbereich Bio und Chemieingenieurwesen, University of Dortmund, 2004.
[8] H. Bock, Randwertproblemmethoden zur Parameteridentifizierung in Systemen nichtlinearer Differentialgleichungen, Dissertation, Bonner Mathematische Schriften, 1987, p. 183.
[9] P. Adam, R. Nicoud, M. Bailly, O. Ludemann-Hombourger, Process and device for separation with variable-length chromatographic columns, US Patent 6,413,419 (2002).